Austin Journal of Analytical & Pharmaceutical Chemistry

Open Access

Austin Publishing Group

Research Article

Potential Antidiabetic Properties of *Syzygium Cumini* (L.) Skeels Leaf Extract-Mediated Silver Nanoparticles

Santosh Mallikarjun Bhavi[1]; Shubha K Mirji[1]; Bothe Thokchom[1]; Sapam Riches Singh[1]; Raju B Maliger[2]; Shivanand S Bhat[3]; Pooja Joshi[1]; BP Harini[4]; Ramesh Babu Yarajarla[1*]; Salim Al Jadidi[2]

[1]Drosophila and Nanoscience Research Laboratory, Department of Applied Genetics, Karnatak University, Dharwad, India

[2]Department of Mechanical and Industrial Engineering (MIE), University of Technology and Applied Science (UTAS), Muscat, Sultanate of Oman

[3]Department of Botany, Smt. Indira Gandhi Government First Grade Women's College, Sagar, India

[4]Department of Zoology, Bangalore University, Bangalore, India

***Corresponding author: Ramesh Babu Yarajarla**
Department of Applied Genetics, Karnatak University, Dharwad, Karnataka – 580003, India.
Email: rameshy@kud.ac.in

Received: January 17, 2024
Accepted: February 17, 2024
Published: February 24, 2024

Abstract

This study explores the use of *Syzygium cumini* (L.) Skeels plant aqueous leaf extract as a reducing agent, which enables the green synthesis and comprehensive characterization of silver nanoparticles (AgNPs). The results indicated that the synthesized AgNPs were spherical in shape with an average size of 27.5 nm and a silver content of approximately 43.18%. The AgNPs exhibited promising antidiabetic and wound-healing properties. The antidiabetic activity, measured through glucose uptake and α–amylase inhibition assays, showed values of 80.08% and 83.91%, respectively. Additionally, the cytotoxicity assessment revealed that the AgNPs exhibited good biocompatibility even at higher doses, indicating their lower toxicity profile. Furthermore, the AgNPs demonstrated wound-closure percentages of 27.59% and 92.48% at 12 h and 24 h respectively, post-treatment, indicating that they were as effective as that of the standard ascorbic acid. These findings suggest that *Syzygium cumini*-mediated AgNPs have significant potential for applications in antidiabetic and wound-healing treatments.

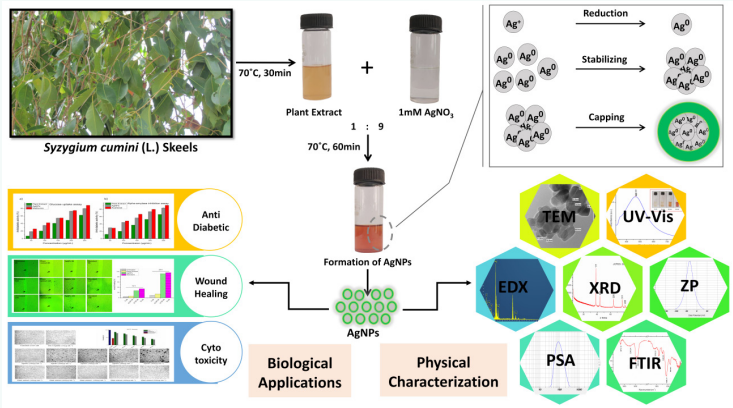

Keywords: Silver nanoparticles; *Syzygium cumini*; Antidiabetic; Wound-healing; Cytotoxicity

Introduction

Diabetes Mellitus (DM) is a complex disease characterized by high blood glucose levels. The primary cause of diabetes is oxidative stress and an increase in Reactive Oxygen Species (ROS) [1]. Untreated diabetes can lead to organ damage, including heart, eyes, and kidneys. There are two main categories of diabetes: impaired insulin secretion and insulin resistance [2]. In spite of the available synthetic drugs, controlling diabetes remains challenging globally [3]. Amylase, an enzyme involved in glucose metabolism, is produced by salivary glands and the pancreas [4]. Current inhibitors of α-amylase and glucosidase used in clinical practice have side effects, limiting their effectiveness in diabetes treatment [5]. Reduced activity of facilitative Glucose Transporters (GLUTs) contributes to insulin resistance and Type II diabetes [6]. Therefore, alternative approaches with fewer side effects are needed. Chronic wounds in individuals with diabetes exhibit impaired healing due to various factors, including hypoxia, dysfunctional cells, impaired angiogenesis, ROS damage, decreased immune resistance, and neuropathy [7,8]. Nanoparticles, especially AgNPs, are becoming increasingly popular due to their various commercial and pharmacological benefits, such as their nano size, which imparts unique physicochemical properties including optical, electrical, and thermal characteristics, as well as high electrical conductivity and biological properties [9]. The properties of AgNPs depend on their size, shape, distribution, and surface characteristics, which can be adjusted by controlling the synthesis process [10]. Green synthesis has emerged as an eco-friendly and sustainable approach to generating nanoparticles, where plant extracts, mi-

Citation: Bhavi SM, Mirji SK, Thokchom B, Singh SR, Maliger RB, et al. Potential Antidiabetic Properties of *Syzygium Cumini* (L.) Skeels Leaf Extract-Mediated Silver Nanoparticles. Austin J Anal Pharm Chem. 2024; 11(1): 1168.

crobes, or enzymes are used as reducing and stabilizing agents. AgNPs synthesized *via* green synthesis have shown promising results in various fields, including antidiabetic applications [11].

Syzygium cumini (L.) Skeels, commonly known as *Syzygium jambolanum* or *Eugenia cumini*, is a widely used medicinal plant in traditional medicine for treating diabetes [12]. Belonging to the Myrtaceae family, it goes by various names including Java Plum, Black Plum, Jambul, Jamun, Jamblang, and Indian Blackberry [13]. This remarkable plant is enriched with a range of beneficial phytochemicals such as flavonoids, terpenoids, and phenolics. It includes compounds such as sitosterol, betulinic acid, crategolic acid, quercetin, myricetin, methylgallate, and kaempferol, which are known for their potential antidiabetic effects [14]. Traditional medicinal system of medication have long recognized the effectiveness of *Syzygium cumini* in treating various health conditions, *viz.* leucorrhea, gastric disorders, fever, piles, wounds, and dental, digestive, and skin disorders [15]. Its historical usage and the presence of these beneficial phytochemicals make *Syzygium cumini* an intriguing natural remedy with potential applications in diabetes treatment.

In the current study, we conducted experiments to examine the potential of green-synthesized AgNPs using *Syzygium cumini* plant extract. We characterized the nanoparticles and assessed their antidiabetic effects, wound-healing properties, and cytotoxicity. Our goal was to explore the diverse biological applications of these nanoparticles in diabetes management.

Methodology

Chemicals and Materials

The study involved the utilization of a range of solvents and chemicals of high quality. These included a precursor solution of 1mM $AgNO_3$, obtained in analytical grade, DMEM media (Dulbecco's Modified Eagle Medium) produced by Sigma Aldrich, MTT reagent (3-(4,5-dimethylthiazolyl-2)-2,5-diphenyltetrazolium bromide), DMSO (Dimethyl Sulfoxide), and Nutrient broth sourced from Hi-media, India. All solvents and chemicals used in the study met the standards of analytical grade quality. Healthy and disease-free leaves of *Syzygium cumini* were collected from an area near the Western Ghat in Karwar, Karnataka, India, at coordinates 14° 53' 57'' N, 74° 07' 49'' E. The plant's identification and authentication were carried out by Dr. Shivanand S. Bhat, Taxonomist at Smt. Indira Gandhi Government First Grade Women's College, Sagar, Karnataka, India (Specimen Acc. No: IGGFWC/Myr-044). The rat myoblast cell line L6 was obtained from the National Centre for Cell Science, located in Pune, Maharashtra, India.

Preparation of Aqueous Leaf Extract

The leaves were meticulously cleaned and subsequently dried in the shade for a few days. Once dried, they were finely ground into coarse powder and kept at room temperature. To prepare the extract, 15g of the coarse powder was mixed with 200 mL of distilled water and heated in a water bath at 70°C for 30 min. The resulting mixture was then filtered using a muslin cloth and Whatman No. 1 filter paper to remove solid particles, yielding a clear extract. This extract was appropriately stored at a temperature of 4°C for future use.

Synthesis of Silver Nanoparticles

The AgNPs were synthesized using a green and eco-friendly method involving the aqueous extract of leaf mixed with a 1 mM $AgNO_3$ solution in a 1:9 ratio. The reaction mixture was kept in the dark at room temperature and incubated in a water bath at 70^{O}C for 1 h, resulting in a color transition from yellow to dark brown. Centrifugation at 10,000 rpm for 12 min and re-dispersion in double distilled water were performed multiple times to remove impurities, and the resulting powder was dried and preserved. This bio-reduction approach utilizing plant extracts offers an environmentally-sustainable and cost-effective alternative for AgNPs synthesis, as reported in previous study [16], and does not involve harmful chemicals, thus making it a pure and eco-friendly process.

Characterization

The green synthesized AgNPs were thoroughly characterized using various techniques in the present study. All characterizations were performed using a single batch of synthesized AgNPs. To confirm the reduction of metal ions to metal in the synthesized AgNPs, UV-Vis spectrophotometry was used, and spectra were measured in the range of 200-800 nm with distilled water used as a blank. To unveil the precise size of the produced AgNPs, X-ray diffraction (XRD) analysis was conducted using a RIGAKU Smart lab SE instrument with Cu_Kα_1D radiation as the source. The diffraction pattern was recorded in the range of 5° to 90° as 2θ angles. Particle size analysis and zeta potential were conducted using a HORIBA SZ-100 instrument to investigate the size distribution, surface charge, and stability of the nanoparticles in colloids. The morphology of the synthesized AgNPs was observed using Transmission Electron Microscopy (TEM) at an accelerating voltage of 120 kV. High-Resolution TEM (HRTEM) images were also obtained using the same TEM instrument (JEOL JEM-2100 PLUS). To investigate the near-surface elements and elemental proportions in the synthesized nanoparticles, Energy Dispersive X-ray Analysis (EDX) was used. The EDX analysis was conducted to determine the elemental composition and distribution of the elements within the nanoparticles. Fourier Transform Infrared (FT-IR) spectrophotometer was utilized to identify the functional groups present in the synthesized nanoparticles. The synthesized silver nanoparticles powder sample was loaded into the FT-IR spectrophotometer and scanned in the range of 400 to 4000 cm^{-1} using the Nicolet iS10 FTIR Spectrophotometer.

Biological Activities

Glucose uptake assay: The glucose uptake assay for AgNPs involved the use of yeast cells as an *in vitro* screening method for hypoglycemic effects. Yeast cells were selected due to the complexity of glucose transport across their cell membrane, which involves facilitated diffusion. To conduct the assay, *Saccharomyces cerevisiae* cells were suspended in distilled water and centrifuged. Different concentrations of the test sample (50, 100, 150, 200 & 250 µg mL^{-1}) were added to test tubes along with glucose. The tubes were incubated at 37°C for 60 min, followed by centrifugation (2500×g.5min), and the concentration of glucose was estimated by determining the absorbance at 540 nm by a spectrophotometer. Metformin was used as a standard drug for comparison.

The % increase in glucose uptake by yeast cells was calculated using the formula:

$$\% \text{ Increase in glucose uptake} = \frac{(\text{Absorbance of control} - \text{Absorbance of test sample})}{(\text{Absorbance of control})} \times 100$$

α-amylase Inhibition Assay: To measure the activity of

α-amylase enzyme, the hydrolysis of starch in the presence of α-amylase enzyme was quantified using 3,5-dinitrosalicylic acid (DNS) reagent. Firstly, samples were mixed with α-amylase and starch in PBS solution, along with different concentrations of the test samples and a standard solution such as Acarbose. The mixture was then incubated at room temperature for 10 min. Control samples were also prepared with and without amylase. To stop the reaction, DNS solution was added to the mixture, and the mixture was boiled in a water bath for 5 min. The absorbance of the resulting solution was measured at 540 nm using a UV-visible spectrophotometer.

The % of enzyme inhibition can be calculated using the formula [17]:

$$\% \text{ of } \alpha\text{-amylase inhibition} = \frac{(\text{Absorbance of control} - \text{Absorbance of test sample})}{(\text{Absorbance of control})} \times 100$$

If the sample extract possesses α-amylase inhibitory activity, the intensity of the color produced by the DNS reagent will be more, indicating a higher percentage of enzyme inhibition.

***In vitro* cytotoxicity:** An MTT assay was employed to evaluate the cytotoxicity of AgNPs and a plant extract on L929 cells. This colorimetric assay measures the reduction of MTT to formazan by mitochondrial dehydrogenases in viable cells. L929 cells were seeded in a 96-well microtiter plate at a density of approximately 10,000 cells per well. Subsequently, the plate was incubated for 24 h, enabling the cells to establish attachment and promote their growth. Different concentrations of the test drug (ranging from 100 to 500 µg mL^{-1} for both extract and AgNPs) were added to the cells, and the plate was incubated for a defined period. Next, 100 µL of 10% MTT reagent was added to each well, and the plate was incubated for 3 h.

The formazan crystals were dissolved in DMSO and their absorbance was measured at 570 nm (with a reference wavelength at 630 nm) using a microplate reader. This enabled the generation of a dose-response curve and determination of the median inhibitory concentration (IC_{50} value). A lower IC_{50} value indicates higher cytotoxicity, while a higher IC_{50} value indicates lower cytotoxicity.

Wound Healing activity by Scratch assay: The wound healing activity of AgNPs and plant extract can be assessed using the Scratch assay, which involves using the L929 cell line. The cells were initially cultured at 37°C in a 5% CO_2 atmosphere for 24 h to allow them to reach ~100% confluence as a monolayer. When performing the Scratch assay, it was assured that the long axis of the tip was always perpendicular to the bottom of the well while scratching across the surface. After scratching, the wells were washed twice with DMEM media and 1X PBS. 25 µL of AgNPs (37.55 µg), plant extract (42.26 µg), and standard ascorbic acid (15 µg), respectively, were added to the wells along with 1 mL of fresh media. It was further incubated at 37°C and observed for wound closure at different time intervals (0 h, 12 h, and 24 h).

Results and Discussion

Ultraviolet-Visible Spectroscopic Analysis (UV-Vis)

Confirmation of AgNPs formation was achieved through UV-Vis spectroscopy measurements. As silver nanoparticles are known to exhibit absorption at wavelengths between 400 to 500 nm [18], the reaction mixture in this study displayed a peak at 465 nm, as shown in Figure 1a, providing conclusive evidence for the presence of AgNPs. UV-Vis spectroscopy serves as a valuable analytical tool for confirming the reduction of Ag^+ to Ag^0 [19].

X-Ray Diffraction Pattern (XRD)

XRD is a commonly used technique to determine the crystal structure of materials, including nanoparticles [20]. In this specific case, XRD was used to determine the crystal structure of synthesized AgNPs. The XRD pattern obtained from the AgNPs sample showed several distinct Bragg reflection peaks located at 2θ angles of 38.10°, 44.29°, 64.47°, 77.39°, and 81.54° (Fiugure 1b), which correspond to lattice planes (1 1 1), (2 0 0), (2 2 0), (3 1 1), and (2 2 2), respectively (JCPDS card number 00-004-0783). Based on the reflection peaks and lattice planes observed, it can be inferred that the AgNPs possess a Face-Centered Cubic (FCC) crystal structure. Furthermore, the XRD pattern indicates that the AgNPs have a well-organized atomic structure and are crystalline in nature with an average size of 27.58 nm. Consequently, the XRD analysis provides significant details on the crystal structure of the synthesized AgNPs and verifies their crystalline nature.

Fourier Transform Infrared (FT-IR) Spectroscopy

The functional groups present on the surface of the AgNPs were evaluated using FT-IR. The spectrum (Figure 1c) revealed peaks at 3673.19 cm^{-1} and 3240.64 cm^{-1}, corresponding to the stretching vibrations of O-H. The peaks at 2986.08 cm^{-1} and 2902.22 cm^{-1} can be attributed to the stretching vibrations of sp^3 and sp^2 C-H bonds respectively [21]. The peaks at 1578.33 cm^{-1} and 1405.73 cm^{-1} can be related to the C=C or C=O stretching vibrations and C-H bending vibrations respectively. While the peaks at 1228.25 cm^{-1}, 1067.31 cm^{-1} and 894.83 cm^{-1} can be ascribed to the stretching vibrations of C-O bonds [22]. As such the AgNPs is functionalized by –OH, $-CH_3$, $=CH_2$, and –CO groups.

Energy Dispersive X-Ray (EDX)

The EDX spectrum (Figure 1d) revealed that the synthesized AgNPs exhibited a strong absorbance peak at approximately 3 keV, which accounted for 43.18% of the constituent silver due to surface plasmon resonance. Additionally, the presence of copper was detected at approximately 1, 8, and 9 keV, constituting 21.54% of the nanoparticles. This is likely attributed to the copper TEM grid used in the analysis, as reported by Bar *et al*. [23]. Carbon and oxygen were also detected as major constituents, constituting 17.54% and 6.55%, respectively, which is consistent with common constituents found in green synthesis methods, as reported by Alsareii *et al*. [24]. Traces of magnesium, silicon, sulphur and calcium were also observed. Overall, the results indicate that the synthesized AgNPs contain a significant amount of silver.

High-Resolution Transmission Electron Microscopy (HR-TEM)

The HRTEM analysis revealed well-resolved lattice fringes in the AgNPs, indicating a well-ordered crystal lattice. By measuring the spacing between these fringes, we obtained a mean particle size of 29.08 nm, which is consistent with the XRD-derived average size. The observed size range of 11.8 nm to 58.4 nm (Figure 2) indicated a distribution of AgNPs with varying dimensions, possibly resulting from different growth rates or agglomeration processes during synthesis. The measured d-spacing values of 0.732 nm, 0.541 nm, and 0.636 nm corresponded to specific crystallographic planes within the FCC structure. The agreement between these measured values and the calculated

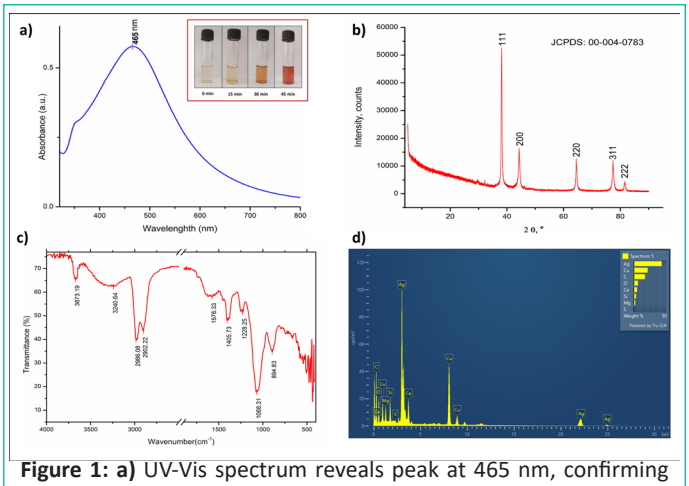

Figure 1: a) UV-Vis spectrum reveals peak at 465 nm, confirming AgNPs formation through color change; **b)** XRD pattern of AgNPs sample displaying prominent peaks at 2θ angles of 38.10°, 44.29°, 64.47°, 77.39°, and 81.54°, indicating the presence of crystalline structures corresponding to lattice planes (1 1 1), (2 0 0), (2 2 0), (3 1 1), and (2 2 2), respectively; **c)** FT-IR spectrum of AgNPs; **d)** EDX analysis confirms silver as the predominant constituent element in the nanoparticles.

lattice parameter from XRD analysis further validated the FCC crystal structure of the AgNPs.

Particle Size Analysis and Zeta Potential

The AgNPs synthesized were analyzed for particle size, with a mean size of 104 nm and a Z-average of 69.5 nm, with Polydispersity Index (PI) value of 0.888, which was calculated based on Brownian motion of the particles (Figure 3a). The zeta potential value was found to be -34.2 mV in our study, indicating that it falls outside the range of -30 mV to +30 mV, which confirms the good stability of the synthesized AgNPs [25]. This indicates that there is a sufficient repulsive force between the particles, preventing them from aggregating and ensuring that they remain stable without colliding with each other in colloidal solution (Figure 3b).

Glucose Uptake Assay

The study selected yeast cells as a model system to evaluate the potential antidiabetic activity of silver nanoparticles due to the presence of at least six members of the glucose transporters family in yeast [26]. In the current study, the ability of AgNPs to stimulate glucose uptake was tested at concentrations ranging from 50 µg mL^{-1} to 250 µg mL^{-1}. A standard drug, metformin, was used for comparison. The results showed that AgNPs were able to stimulate glucose uptake in yeast cells in a dose-dependent manner. At 50 µg mL^{-1} AgNPs stimulated glucose uptake by 18.95%, and this increased to 80.08% at 250 µg mL^{-1} (Figure 4a). In comparison, metformin stimulated glucose uptake by 26.03% at 50 µg mL^{-1} and 88.51% at 250 µg mL^{-1}. The IC_{50} values were also calculated for the three test compounds. These values represent the concentration of the compound required to stimulate 50% of glucose uptake. The IC_{50} value for AgNPs was found to be 142.48 µg mL^{-1}, compared to 126.64 µg mL^{-1} for metformin. For plant extract, the percentage of glucose uptake at 50 µg mL^{-1} was found to be 7.10%, and at 250 µg mL^{-1} it was 62.51%, with an IC_{50} value of 200.23 µg mL^{-1}. In comparison with the plant extract, AgNPs and metformin demonstrated higher percentages of glucose uptake at all concentrations tested. Additionally, the IC_{50} value for AgNPs was lower than that of the plant extract, indicating that AgNPs were more effective in stimulating glucose uptake in yeast cells. These results suggest that AgNPs have the potential to be a promising plant-based antidiabetic agent, as they demonstrated comparable or even higher activity in stimulating glucose uptake compared to the standard drug metformin, and were more effective than the plant extract.

α-amylase Inhibition Assay

The study aimed to assess the potential antidiabetic activity of silver nanoparticles by evaluating their ability to inhibit α amylase, an enzyme responsible for carbohydrate breakdown. Earlier research by Saratale *et al*., (2018) has reported that green-synthesized silver nanoparticles have the capability to lower blood glucose levels by inhibiting α-amylase activity [27]. Building upon synthesized AgNPs and plant extracts were tested at concentrations of 50 µg mL^{-1} to 250 µg mL^{-1}, alongside a standard drug acarbose was tested at the same concentrations for comparison (Figure 4b). The IC_{50} value for acarbose was found to be 107.58 µg mL^{-1}, while for AgNPs, it was 121.21 µg mL^{-1} and for plant extract, it was 193.29 µg mL^{-1}. Both AgNPs and acarbose, as well as plant extract, exhibited a dose-dependent increase in the percentage of inhibition of α-amylase activity. The percentage of inhibition for AgNPs ranged from 30.01% to 83.91%, for plant extract it ranged from 11.98% to 66.31%, and for acarbose, it ranged from 29.17% to 91.14%. Although AgNPs and plant extract did not surpass acarbose in terms of percentage of inhibition, however, the AgNPs was found to be very close to the inhibition percentage of the standard drug. These results suggest that AgNPs hold potential as an antidiabetic agent, as they exhibited comparable inhibitory activity against α-amylase in comparison to the standard drug. Overall, the study showed promising results for the potential use of AgNPs as an alternative treatment for diabetes.

In vitro Cytotoxicity Activity

The study employed the MTT assay to evaluate the viability and cytotoxicity of L929 fibroblast cells when exposed to AgNPs and a plant extract. Both plant extract and AgNPs exerted

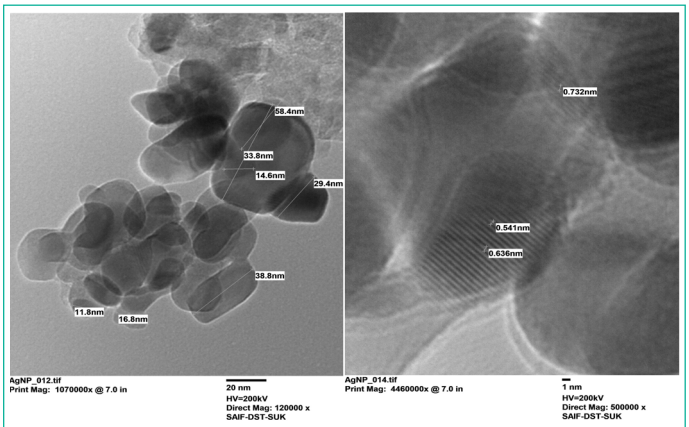

Figure 2: High-resolution TEM reveals exquisite details of AgNPs, showing their uniform distribution and average size of 29.08 nm with an average lattice fringes as 0.636 nm.

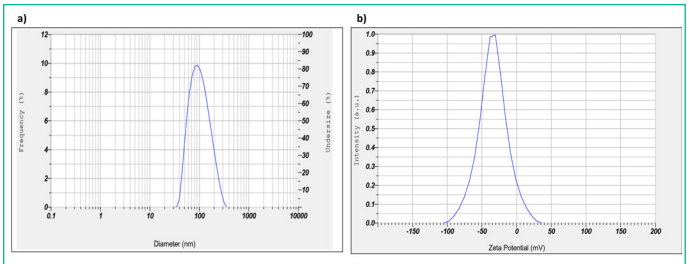

Figure 3: a) The measurement of results obtained from a particle size analyzer, indicating a diameter of the AgNPs to be < 100nm; **b)** Zeta Potential Analysis measures AgNPs reveals a mean charge of -34.2 mV, indicating a negatively charged surface.

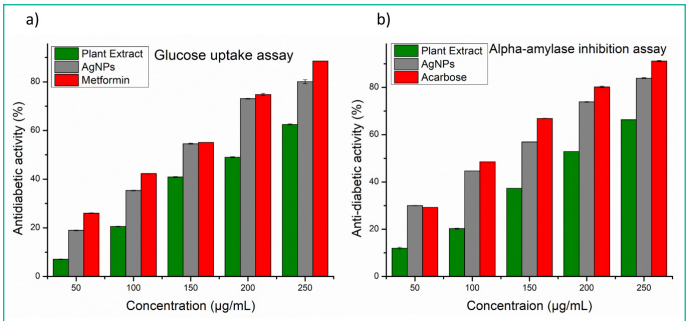

Figure 4: a) The antidiabetic activities of synthesized AgNPs were estimated using Glucose uptake assay; **b)** The antidiabetic activities of synthesized AgNPs were estimated using α-amylase inhibition.

concentration-dependent effects on cell viability. At a concentration of 100 µg mL^{-1}, the cell viability was recorded as 86.39% and 78.58%, which gradually decreased to 40.12% and 36.71% at 500 µg mL^{-1} for plant extract and AgNPs respectively. In comparison, treatment with the standard drug Cisplatin at 15 µg mL^{-1} resulted in a cell viability of 45%. The IC_{50} value for plant extract and AgNPs were calculated to be 422.61 µg mL^{-1} and 375.55 µg mL^{-1} respectively (Figure 5).

Remarkably, the cytotoxic effects of both the plant extract and AgNPs were observed at a significantly higher concentration of 500 µg mL^{-1}, indicating their relatively low toxicity compared to the standard drug Cisplatin, which exhibited cytotoxicity at a much lower concentration of 15 µg mL^{-1}. As a result, for future biomedical application studies, concentrations as high as 100 µg mL^{-1} can be safely utilized for both the plant extract and AgNPs without causing substantial cytotoxic effects. These findings underscore the potential of the plant extract and AgNPs in diverse biomedical applications, highlighting their favorable safety profile and suggesting their suitability as alternatives to Cisplatin.

Wound-Healing Activity

Ascorbic acid is involved in all phases of wound healing. In the inflammatory phase, it is required for neutrophil apoptosis and clearance, while in the proliferative phase, ascorbic acid contributes towards synthesis, secretion, maturation, and degradation of collagen [28]. The activity of wound healing was evaluated by measuring the percentage of wound healing closure at 12 h and 24 h after treatment with different concentrations of untreated, standard ascorbic acid, plant extract, and AgNPs.

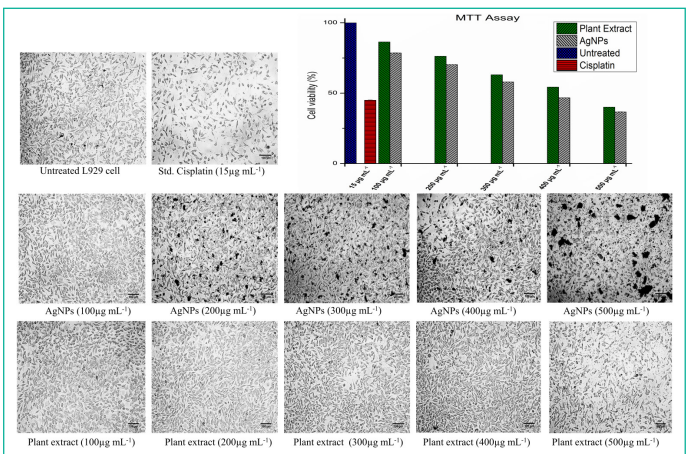

Figure 5: Cell viability of the standard, untreated, plant extract and AgNPs at concentrations ranging from 100 µg mL^{-1} to 500 µg mL^{-1} for both the plant extract and AgNPs. For the standard, the concentration is 15 µg mL^{-1}. The graph illustrates the cytotoxicity effect against different concentrations of the plant extract and AgNPs.

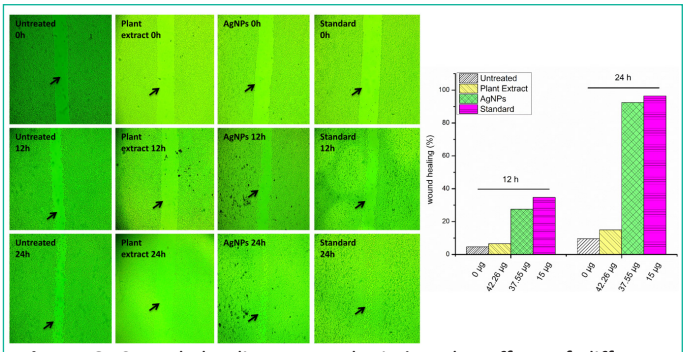

Figure 6: Scratch healing assay depicting the effect of different treatments on wound closure. Untreated samples, plant extract, AgNPs, and standard ascorbic acid were applied at concentrations of 0 µg, 15 µg, 42.26 µg, and 37.55 µg. The graph displays the healing progress at 12-24 h.

The concentrations used in the study (0 µg, 15 µg, 42.26 µg, and 37.55 µg) were specifically chosen as they represent the 10% of the IC_{50} value obtained in an MTT assay. This is to minimize cytotoxicity while evaluating the wound healing potential. At 12 h post-treatment, the percentage of wound-healing closure was found to be 4.581% for untreated, 34.76% for standard ascorbic acid, 6.54% for plant extract, and 27.59% for AgNPs. At 24 h post-treatment, the percentage of wound-healing closure was found to be 9.60% for untreated, 96.48% for standard ascorbic acid, 14.98% for plant extract and 92.48% for AgNPs (Figure 6). These results suggest that all the treatments showed some degree of wound healing activity, with the standard ascorbic acid and AgNPs treatments showing the most significant improvement in wound-healing closure at both 12 h and 24 h post-treatment.

In recent research, synthesized AgNPs have demonstrated impressive potential in promoting wound-healing. These AgNPs stimulate the proliferation and migration of fibroblast cells [29], as observed in scratch assays. They actively induce fibroblast cells to proliferate and migrate towards the wound site, leading to increased cell mass. Additionally, the AgNPs trigger the differentiation of fibroblast cells into myofibroblasts, further enhancing cell migration and wound contraction [30].

These findings suggest that the synthesized AgNPs possess powerful wound healing properties, including the ability to induce the "fibroblast-to-myofibroblast transition." Furthermore, *in vitro* studies using L929 cell lines have shown significant wound-healing efficacy, with increased fibroblast cell proliferation, migration, and wound-contraction induced by the AgNPs [31]. This shows the enormous potential of AgNPs as a promising new strategy for wound- healing.

Conclusion

The overall study suggests that *Syzygium cumini* (L.) Skeels leaves can serve as natural agents for the synthesis of AgNPs, which show promise as agents for diabetes treatment. The synthesized AgNPs possess a crystalline structure, spherical shape, and vary in size from 27.5 nm to 69.5 nm. They exhibit impressive wound-healing capacity, suggesting their potential application in diabetes treatment. Furthermore, plant-based synthesis of silver nanoparticles offers a safe and advantageous approach, free from toxic chemicals with natural capping agents. Both extracts and nanoparticles display dose-dependent antidiabetic activity, with the nanoparticles demonstrating superior performance. Further research is needed to uncover the molecular mechanisms and explore the medical applications of these nanoparticles.

Author Statements

Acknowledgments

The authors would like to express their sincere gratitude to the DST PURSE Phase-II Program and the University Scientific Instrumentation Centre (USIC) of Karnatak University, Dharwad, as well as the Sophisticated Analytical Instrument Facility (SAIF) at Shivaji University, Kolhapur, for their instrumental support. Special thanks are also extended to the National Centre for Cell Science, Pune, Maharastra, India, for providing the L929 cell line. Additionally, the authors express their gratitude to the Department of Applied Genetics, Karnatak University, Dharwad, for providing the necessary research facilities. These contributions have greatly facilitated the progress and success of this research project.

Author Contributions

Salim Al Jadidi: Critical Review and Editing.

Santosh Mallikarjun Bhavi: Conceptualization, Methodology, Supervision, Investigation, Software usage, Roles/Writing-review & editing.

Shubha K. Mirji: Conceptualization, Methodology, Investigation, Roles/Writing- original draft.

Bothe Thokchom: Investigation, Software usage, Data curation, Roles/Writing- review & editing.

Sapam Riches Singh: Formal analysis, Data curation, Roles/Writing- review & editing.

Raju B. Maliger: Methodology, critical review & corrections of manuscript

Shivanand S. Bhat: Resources,Validation, Roles/Writing- review & editing.

Pooja Joshi: Roles/Writing- review & editing.

B. P. Harini: Formal analysis, Roles/Writing- review & editing.

Ramesh Babu Yarajarla: Resources, Project administration, Validation, Supervision, Roles/Writing- review & editing.

Declaration of Competing Interest

The authors declare that there is no conflict of interest.

Funding

Academic Publication Charges (APC) for this research is funded by Dr. Salim Al Jadidi, University of Technology and Applied Sciences (UTAS), Muscat, Oman.

Referenes

1. Kharroubi AT. Diabetes mellitus: The epidemic of the century. World J Diabetes. 2015; 6: 850.
2. Halayal RY, Bagewadi ZK, Maliger RB, Al Jadidi S, Deshpande SH. Network pharmacology based anti-diabetic attributes of bioactive compounds from Ocimum gratissimum L. through computational approach. Saudi J Biol Sci. 2023; 30: 103766.
3. Dowarah J, Singh VP. Anti-diabetic drugs recent approaches and advancements. Bioorg Med Chem. 2020; 28: 115263.
4. Kaur N, Kumar V, Nayak SK, Wadhwa P, Kaur P, Sahu SK. Alpha-amylase as molecular target for treatment of diabetes mellitus: A comprehensive review. Chem Biol Drug Des. 2021; 98: 539–60.
5. Oyedemi SO, Oyedemi BO, Ijeh II, Ohanyerem PE, Coopoosamy RM, Aiyegoro OA. Alpha-Amylase Inhibition and Antioxidative Capacity of Some Antidiabetic Plants Used by the Traditional Healers in Southeastern Nigeria. Sci World J. 2017; 1–11.
6. Chadt A, Al-Hasani H. Glucose transporters in adipose tissue, liver, and skeletal muscle in metabolic health and disease. Pflüg Arch - Eur J Physiol. 2020; 472: 1273–98.
7. Falanga V. Wound healing and its impairment in the diabetic foot. The Lancet. 2005; 366: 1736–43.
8. Guo S, DiPietro LA. Factors Affecting Wound Healing. J Dent Res. 2010; 89: 219–29.
9. Zhang X-F, Liu Z-G, Shen W, Gurunathan S. Silver Nanoparticles: Synthesis, Characterization, Properties, Applications, and Therapeutic Approaches. Int J Mol Sci. 2016; 17: 1534.
10. Khan I, Saeed K, Khan I. Nanoparticles: Properties, applications and toxicities. Arab J Chem. 2019; 12: 908–31.
11. Rafique M, Sadaf I, Rafique MS, Tahir MB. A review on green synthesis of silver nanoparticles and their applications. Artif Cells Nanomedicine Biotechnol. 2017; 45: 1272–91.
12. Ayyanar M, Subash-Babu P. Syzygium cumini (L.) Skeels: A review of its phytochemical constituents and traditional uses. Asian Pac J Trop Biomed. 2012; 2: 240–6.
13. Swami SB, Thakor NSJ, Patil MM, Haldankar PM. Jamun (Syzygium cumini (L.)): A Review of Its Food and Medicinal Uses. Food Nutr Sci. 2012; 03: 1100–17.
14. Srivastava S, Chandra D. Pharmacological potentials of Syzygium cumini : a review: Pharmacological potentials of Syzygium cumini. J Sci Food Agric. 2013; 93: 2084–93.
15. Jagetia GC. Phytochemical Composition and Pleotropic Pharmacological Properties of Jamun, Syzygium Cumini Skeels. J Explor Res Pharmacol. 2017; 2: 54–66.
16. Logeswari P, Silambarasan S, Abraham J. Synthesis of silver nanoparticles using plants extract and analysis of their antimicrobial property. J Saudi Chem Soc. 2015; 19: 311–7.
17. Balan K, Qing W, Wang Y, Liu X, Palvannan T, Wang Y, et al. Antidiabetic activity of silver nanoparticles from green synthesis using Lonicera japonica leaf extract. RSC Adv. 2016; 6: 40162–8.
18. Agustina TE, Handayani W, Imawan C. The UV-VIS Spectrum Analysis From Silver Nanoparticles Synthesized Using Diospyros maritima Blume. In: Leaves Extract: Presented at the 3rd KOBI Congress, International and National Conferences (KOBICINC 2020. Bengkulu, Indonesia. 2021.
19. Rani P, Kumar V, Singh PP, Matharu AS, Zhang W, Kim K-H, et al. Highly stable AgNPs prepared via a novel green approach for catalytic and photocatalytic removal of biological and non-biological pollutants. Environ Int. 2020; 143: 105924.
20. Malathi G, Valliammai T, Begum R, Vinayaka KS, Udappusamy V, Nirmala P, et al. Green Synthesis of Electrochemically Active Silver Nanoparticles. Orient J Chem. 2023; 39: 82–94.
21. Thokchom B, Bhavi SM, Abbigeri MB, Shettar AK, Yarajarla RB. Green synthesis, characterization and biomedical applications of Centella asiatica-derived carbon dots. Carbon Lett. 2023; 33: 1057-1071.
22. Karimi S, Feizy J, Mehrjo F, Farrokhnia M. Detection and quantification of food colorant adulteration in saffron sample using chemometric analysis of FT-IR spectra. RSC Adv. 2016; 6: 23085–93.
23. Bar H, Bhui D, Sahoo GP, Sarkar P, De SP, Misra A. Green synthesis of silver nanoparticles using latex of Jatropha curcas. Colloids Surf Physicochem Eng Asp. 2009; 339: 134–9.

24. Alsareii SA, Manaa Alamri A, AlAsmari MY, Bawahab MA, Mahnashi MH, Shaikh IA, et al. Synthesis and Characterization of Silver Nanoparticles from Rhizophora apiculata and Studies on Their Wound Healing, Antioxidant, Anti-Inflammatory, and Cytotoxic Activity. Molecules. 2022; 27: 6306.

25. Joseph E, Singhvi G. Multifunctional nanocrystals for cancer therapy: a potential nanocarrier. In: Nanomaterials for Drug Delivery and Therapy Elsevier. 2019; 91–116.

26. Roy A, Dement AD, Cho KH, Kim J-H. Assessing Glucose Uptake through the Yeast Hexose Transporter 1 (Hxt1. PLOS ONE. 2015; 10: 0121985.

27. Saratale RG, Shin, Kumar G, Benelli G, Kim D-S, Saratale GD. Exploiting antidiabetic activity of silver nanoparticles synthesized using Punica granatum leaves and anticancer potential against human liver cancer cells (HepG2. Artif Cells Nanomedicine Biotechnol. 2018; 46: 211–22.

28. Moores J. Vitamin C: a wound healing perspective. Br J Community Nurs. 2013; 18: 6–11.

29. Fiedler G, Schneider C, Igbinosa EO, Kabisch J, Brinks E, Becker B, et al. Antibiotics resistance and toxin profiles of Bacillus cereus-group isolates from fresh vegetables from German retail markets. BMC Microbiol. 2019; 19: 250.

30. Lakkim V, Reddy MC, Pallavali RR, Reddy KR, Reddy CV, Inamuddin B, et al. Green Synthesis of Silver Nanoparticles and Evaluation of Their Antibacterial Activity against Multidrug-Resistant Bacteria and Wound Healing Efficacy Using a Murine Model. Antibiotics. 2020; 9: 902.

31. Paladini F, Pollini M. Antimicrobial Silver Nanoparticles for Wound Healing Application: Progress and Future Trends. Materials. 2019; 12: 2540.